Effect of the Stator Slot Indents on Fluid Damping Loss in Submersible Pump Applications

Didem Tekgun
Dept. of Electrical & Electronics Engineering
Abdullah Gul University
Kayseri, TURKEY
didem.tekgun@agu.edu.tr

Muhammed Muhsin Cosdu
Dept. of Electrical & Electronics Engineering
Abdullah Gul University
Kayseri, TURKEY
muhammedmuhsin.cosdu@agu.edu.tr

Burak Tekgun
Dept. of Electrical & Electronics Engineering
Abdullah Gul University
Kayseri, TURKEY
burak.tekgun@agu.edu.tr

Irfan Alan
Dept. of Electrical & Electronics Engineering
Abdullah Gul University
Kayseri, TURKEY
irfan.alan@agu.edu.tr

2022 4th Global Power, Energy and Communication Conference (GPECOM) | 978-1-6654-6925-8/22/$31.00 ©2022 IEEE | DOI: 10.1109/GPECOM55404.2022.9815636

***Abstract*—In this study, the effect of fluid damping on the performance of a 2-pole, 4-kW line start synchronous reluctance machine (LS-SynRM) with different slot opening structures for submersible water pump applications is investigated. Since the submersible pump motors run inside a fluid-filled environment and the fluid viscosity and density differ from the air, it causes an increased damping effect comparing air-filled machines. Hence, a non-negligible damping loss occurs. In this study, the damping effects of the fluids in a 24 slot LS-SynRM for various stator slot indentations are investigated with computational fluid dynamics (CFD) finite element analysis (FEA) to highlight the importance of the fluid damping loss in flooded machines. Results show that the damping loss can go as high as 10% of the motor output power when the stator surface has indentations, and this loss can be cut down to 3.5 % when the surface indentations are eliminated with custom no-slotting wedge structures.**

Keywords— submersible water pumps, line start synchronous reluctance machine, stator slot indents, computational fluid dynamics, fluid damping loss

I. Introduction

Today, reducing energy losses has become a common goal worldwide for preserving natural sources and reducing energy costs. Considering the electric drive systems constitute 70 % of the global energy consumption, improving electric machine efficiencies provides important nationwide and global scale advantages [1]. Among the electric motors used in the industry, a major portion belongs to pump motors used for pumping underground waters and petroleum products. Generally, the motors used in the submersible pump applications run at very low-efficiency levels because of the cost considerations, motor design issues, and wrong selection of motor-pump configurations. Due to the features like robustness, low cost, line start capability, Induction Machines (IM) are generally the first choice for pump applications.

However, the IMs operate with low efficiency, especially at low and medium power levels [2]. Permanent magnet synchronous machines (PMSM) are powerful rivals to the IM as they have higher power density and better efficiency compared to IM. Although PMSM with drive systems are not preferred in submersible pump applications due to their cost, Line Start PMSM (LS-PMSM) can be found commercially as their initial cost is relatively lower due to the elimination of the drive cost. LS-PMSM with different type of rotor structure is a typical solution to increase the efficiency of the motor compared to the IMs [3], [4]. The LS-PMSM combines the advantages of robustness and line-start capability of IMs and high-power factor (PF), torque density and therefore high efficiency of PM motor. A 4-pole LS-PMSM is proposed for a submersible water pumping application in [5]. Since the rare-earth permanent magnet material is inserted to rotor, the overall cost of the machine is increased. A high performance, LS-PMSM is proposed for pumping application in [6]. It uses a 2-pole rotor geometry and the rotor cage is designed to find minimum starting current. In [7], the curved shape PM with powder hybrid rotor is proposed and the analysis is concluded that this rotor configuration has a better efficiency and PF which is a good alternative for high duty applications like fans, pumps, and compressors instead of IMs. Nonetheless, problems like demagnetization during start-up through line voltage and having high costs and external dependence on rare earth elements lead researchers to find new alternatives to these motors.

Synchronous reluctance motors (SynRM) can also reach high-efficiency levels and are also being a good alternative to the IM. Yet they require a power electronic drive similar to the PMSM. Therefore, a hybrid technology called Line Start SynRM (LS-SynRM) that combines the features of squirrel cage IM and SynRM come to the scene as a reasonable alternative to the IMs by having the line start capability and not having rare earth permanent magnets as well. LS-SynRM starts as an IM due to the conductor bar structure inserted into the rotor. After reaching the synchronous speed, it runs as a SynRM merely relying on saliency torque that is due to the flux barriers on the rotor. While operating at synchronous speed, there would be no induced currents in rotor bars leading to zero loss at conductor bars. Besides, SynRMs have higher power and torque density compared to the IMs [3]. Therefore, LS-SynRM is a very attractive alternative that is reliable, efficient, and low-cost compared to high-cost PMSM and low-efficiency IM.

Although the discovery of SynRM dates back to 1923 [8], the first LS-SynRM was designed in 2003 [9]. In the literature, limited research can be found related to SynRM being a submersible water pump motor. A 2-pole, 5 HP multi-barrier LS-SynRM is proposed for a 6-inch bore-well submersible water pump in [10]. Here, two different type of rotor structure namely; Rotor-A and Rotor-B; are designed to have high saliency. The flux barriers of both rotors are filled with Aluminum which acts as cage bars. Rotor-B has three flux barriers like the Rotor-A with an additional cage inserted to the d-axis of the Rotor-B. The analysis results showed that the both rotor structure are capable of achieving improved saliency ratio. It is also observed that only Rotor-B can be synchronized under five times of the rotor inertia due to the additional cage. A 2-pole, 3 kW LS-SynRM with two different rotor flux barrier design is proposed in [11] for fan and pump applications. In this study, transient and steady state performance of the 3 and 4 flux barrier rotor

978-1-6654-6925-8/22/$31.00 ©2022 IEEE

configurations are discussed and FEA analysis linked with an optimization algorithm showed that the 4-flux barrier rotor design has slightly better performance. Die-cast aluminum is used to fill some of the flux barrier to perform the line start feature. Analysis showed that the IE2 class IM efficiency is upgraded to IE4 class with 4-Flux barrier LS-SynRM. In [12], 2-pole, 3.7 kW multi-barrier line-start ferrite assisted synchronous reluctance motor is proposed for a submersible water pump application. Similar to the studies mentioned above, the aim was a solution to replace an improved and efficient motor design instead of poor efficiency IMs. Here, ferrite assisted arc shaped flux barrier rotor design is employed to minimize torque while maximizing the torque per ampere. The reluctance torque is considered as the main torque producer due to the flux barrier and the aim to use the ferrite magnets is to improve the PF with minimum magnet volume. Results showed that the motor efficiency is improved to IE4 standards. Recently, two different studies are proposed for submersible water pump motor application; the one with 4 pole and solar PV fed SynRM [13], and the other is 2 pole ferrite magnet assisted LS-SynRM [14]. In [13], a 2.2 kW, 4 pole synchronous reluctance motor is designed using combined analytical and FEA design. Then, a comparison study is given and the results show that 40% of IM losses are eliminated and the efficiency is improved by 3-4%.[14] proposes a 2 pole, 3.7 kW ferrite-assisted LS-SynRM. Here, the optimum number and width of flux barriers are found by the trial-and-error method. The numbers of flux barriers analyzed are two, three, and four; and the barrier widths vary from 2 to 5.5 mm. According to the results, the highest saliency ratio is obtained when the number of flux barriers is 3 and the width of each barrier is 4 mm.

In the literature there exist limited research related to the submersible pump applications. Moreover, the research interest in this field is shifted to the line start synchronous machines, especially the LS-SynRM, since they are reliable, cheap and efficient alternatives of the IM. It is a fact that running the LS-SynRM both in asynchronous and synchronous modes is a tedious process. The possible problems such as the inability to synchronize and crawling have to be investigated carefully. To perform the synchronization capability analysis, mechanical dynamics like the moment of inertia and friction and windage torque should be known. Unlike typical applications, the submersible pump motors run inside fluid-filled environments where they are also filled with fluid to avoid the water to be pumped leaking into the motor. Hence, it operates while the stator and rotor are flooded. Therefore, similar to the windage loss in the air-filled machines, damping loss occurs in the flooded machines due to the damping effect of the fluid. All the aforementioned studies in the literature assume the damping loss can be neglected similar to the windage loss. Also, the synchronization analysis is done by the fluid damping effect is ignored and total motor and load moment of inertia is assumed to be 3 to 5 times bigger that the calculated value [12]. However, the damping loss should not be neglected as any fluid is denser than the air and it causes more loss compared to the windage loss and effects the acceleration dynamics and synchronization performance during the machine design stage.

In this study, a 2-pole, 4 kW LS-SynRM as a submersible water pump motor which is designed and optimized in [15] is employed. Unlike the above studies related to the submersible water pump applications, the fluid damping loss is analyzed using computational fluid dynamics (CFD) finite element analysis (FEA) for various slot opening structures by placing different wedge shapes and no wedge placed in the slot openings. It is aimed to investigate the fluid damping effects to show how the damping loss varies with the different stator indentation structures in flooded electric machines.

Here, two indented and a smooth stator surface area are investigated in terms of water damping loss. First, the design without any wedge insertion to the slot openings of the stator with large-indented area is analyzed. This way, the damping loss recorded as 386.2 W at steady-state conditions. Second, standard wedge is inserted to slot openings. Since the slot openings are larger than usual in submersible pump motors, even the standard wedge is inserted in the slots, indents exist on the stator surface as well. Although the area of the indents is smaller than the first design, damping loss recorded as 362 W, similar to the no wedge structure. Lastly, a custom wedge structure which allows to close all the indents and create a smooth surface on the air gap side of the stator is inserted to the slots and damping loss is analyzed. A dramatic reduction on the damping loss is observed which is recorded as 139.9 W at steady state operation of the machine. The analysis is also performed assuming that the fluid is replaced with air and for this case the windage loss is calculated not more than a couple watts. Comparing with the fluid damping losses the windage loss is negligible. Hence, it is concluded that the fluid damping loss cannot be assumed as windage loss and cannot be ignored for the flooded machines.

Rest of the paper is organized as follows: First, background information about the fluid damping effects is provided in Section II. Second, analysis results of different slot opening structures with different indents on the stator surface and a comparison study are presented in Section III. Lastly, a brief conclusion is given in Section IV.

II. Fluid Damping Loss Analysis

Submersible water pump motors have flooded stators and rotors where the fluid is usually a mixture of water and polypropylene glycol. Damping loss occurs while the rotor is rotating in the fluid like the windage losses in air-cooled motors. As the water mixture is denser than the air, it is expected to yield more loss compared to the windage loss. The related analytical calculations are as follows [16]:

$$P_w = C_d \rho \pi r^4 \omega^3 L \qquad (1)$$

where P_w is the damping loss, C_d is the skin friction coefficient, ρ is the density of the fluid, r is the radius of the rotor, ω is the angular velocity and L is the rotor length. Here, skin friction coefficient C_d is calculated as:

$$C_d = \frac{F_d}{qA} = \frac{F_d}{\frac{1}{2}\rho v^2 A} \qquad (2)$$

where F_d is the drag force, q is dynamic pressure, A is the projected area of the rotor, and v is the velocity of the fluid.

On the other hand, these properties can only be calculated numerically using an CFD FEA. Considering the different type of slot opening structures the analyses are carried out and details of the analyses are given in the following section.

III. Analysis with Different Slot Opening Structures

Since the submersible water pumps have fluid-filled structures, mostly, Polyvinyl Chloride (PVC) insulated magnet wire is preferred. PVC is suitable for applications where the cables exposed fluids. Since its chemical stability is higher than the standard copper wire, it is safe and appropriate to use PVC wire for the flooded environments. PVC wire diameters are usually larger than the standard magnet wires due to the thick insulation layer. Therefore, slot openings of the submersible pump motor stators are designed to be larger than standard industrial motor stators. Although standard wedges are inserted to the slot openings to keep the coils inside the slot during the operation, they create an indented surface on the airgap side of the stator. The structure with intends cause more liquid fluctuations as shown in Fig. 1 at the surface and it ends up with dramatically increased damping loss accordingly.

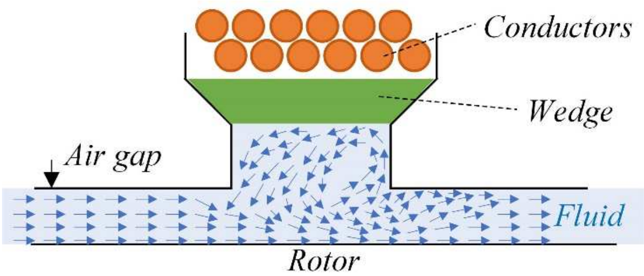

Fig. 1. Liquid flow in the airgap cavity.

In this study, damping loss is investigated through CFD analysis for designs with no wedge, standard wedge and customized no-slotting wedge structures.

A. Analysis with No Wedge

In this structure, there is no wedge inserted in the slots, so, the liquid in the airgap can go through the windings from the slot openings as shown in Fig. 2. In order to calculate the fluid damping loss using (1), two parameters are required to be obtained through CFD analysis, which are the drag force and dynamic pressure so that the skin friction coefficient can be calculated using (2). The 3D fluid body structure used in the CFD analysis is illustrated in Fig. 3.

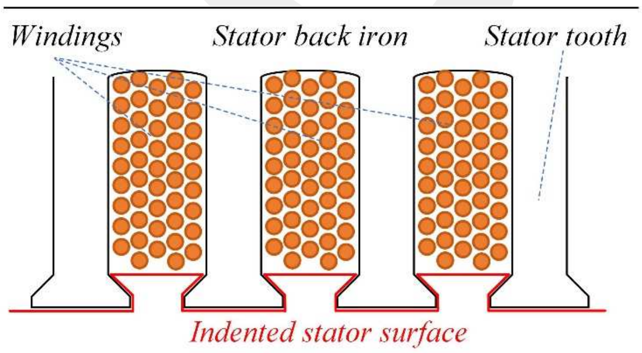

Fig. 2. Indented stator surface with no wedge inserted into the stator slots.

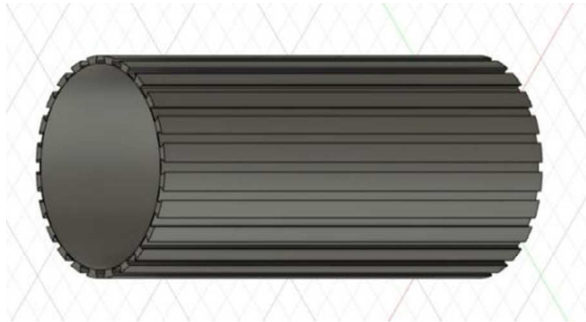

Fig. 3. 3D fluid body geometry with coil slot.

According to the analysis results presented in Table I, the damping loss varied between 0.155 W and 386.2 W, as the rotor speed varies between 500 rpm and 3000 rpm. It can be clear from the results that the damping loss increases exponentially with the speed. Considering that the motor used in the case study has 4 kW output power, almost 10% loss is associated with the fluid damping loss.

TABLE I. Fluent Analysis Results of the No Wedge Geometry

Speed (Rpm)	Skin Friction Coefficient (Cd)	Damping Loss (W)
500	0.0168	0.155
1000	0.0182	17.28
1500	0.0196	53.36
2000	0.0194	117.2
2500	0.0186	228.7
3000	0.0251	386.2

B. Analysis with Standard Wedge

Here, standard wedges are inserted to the stator slot openings to keep the coils inside the slot as shown in Fig. 4. The 3D fluid body structure used in the CFD analysis for this slot opening structure is given in Fig. 5. As it can be observed from these figures, indents of the structure with standard wedges are smaller than the previously presented no-wedge structure. Hence, water fluctuation on the indents is less than the no wedge structure and accordingly, the damping losses are smaller compared to the no-wedge form. CFD analysis results are listed at Table II. According to the analysis results, at the lowest loss is 0.138 W at 500 rpm and the highest loss is 362.0 W at 3000 rpm which is slightly better than the no-wedge structure.

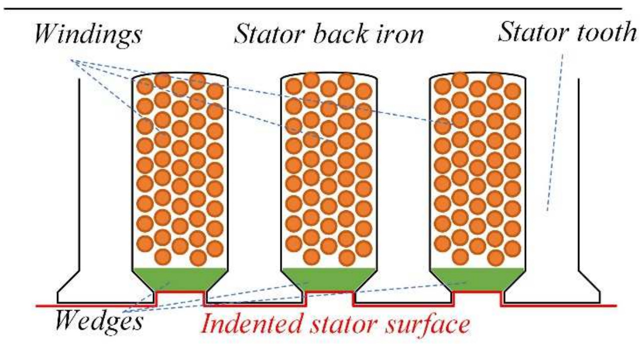

Fig. 4. Indented stator surface with standard wedges inserted into stator slots.

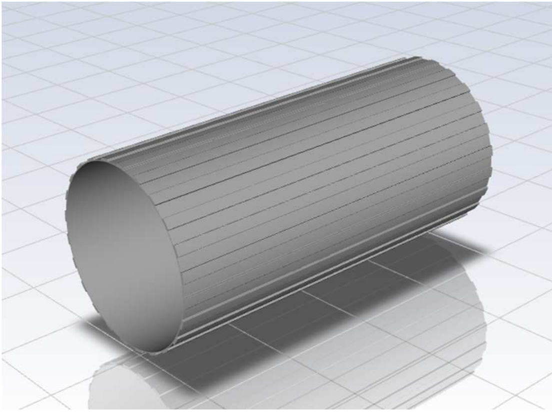

Fig. 5. 3D fluid body geometry with standard wedge structure.

TABLE II. FLUENT ANALYSIS RESULTS OF THE STANDARD WEDGE GEOMETRY

Speed (Rpm)	Skin Friction Coefficient (Cd)	Damping Loss (W)
500	0.0176	0.138
1000	0.0196	13.33
1500	0.0201	46.15
2000	0.0194	105.6
2500	0.0194	206.2
3000	0.0190	362.0

C. Analysis with Custom No-Slotting Wedge

Here, it is aimed to close the slot openings completely with a customized wedge structure insertion as illustrated in Fig. 6. The 3D fluid body structure used in the CFD analysis for the smooth slot surface structure is given in Fig. 7. This way smoothness of the stator inner surface is maximized and indents are disappeared. Hence, fluid surrounding the rotor structure slides on a smooth surface and this results in a significant reduction in damping loss.

Table III. shows the results with customized no-slotting wedge structure. According to the results, the lowest loss is recorded as 0.138 W at 500 rpm and the highest is the 139.9 W at 3000 rpm which is almost 3 times better than the standard-wedge structure.

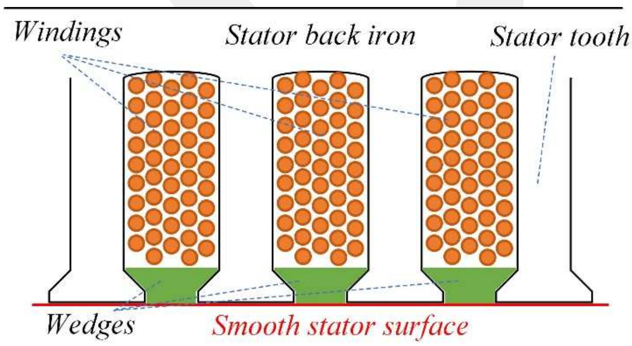

Fig. 6. Smooth stator surface with custom no-slotting wedges inserted into the stator slots.

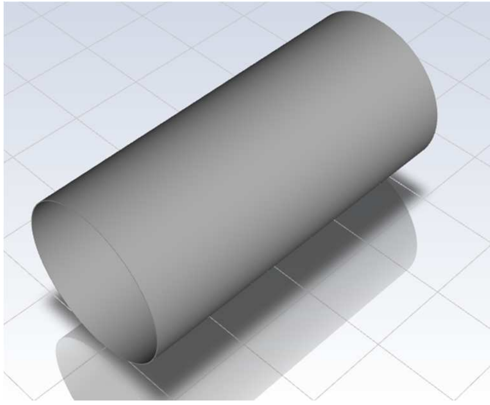

Fig. 7. 3D fluid body geometry with custom no-slotting wedge structure.

TABLE III. FLUENT ANALYSIS RESULTS OF THE NO SLOT GEOMETRY

Speed (Rpm)	Skin Friction Coefficient (Cd)	Damping Loss (W)
500	0.0135	0.110
1000	0.0121	8.230
1500	0.0109	25.01
2000	0.00985	53.58
2500	0.00913	96.99
3000	0.00866	139.9

D. Comparison and Discussion

According to this analysis one can conclude that the damping loss is at its minimum when there are no indents on the stator surface, and it increases dramatically even with small surface indents. The depth of the indents effects the damping loss, but the loss variation is slight comparing with the loss on the smooth surface.

A summary and a comparison of the losses associated to the slot opening structures are presented at Table IV. Additionally, the scenario; which ignores the damping loss of the fluid-filled motor and assumes that the machine works as in the air; is analyzed and the results are included to the comparison given in Table IV. Since the density of the fluid (mixture of water and polypropylene glycol) filled inside the motor is 998.2 kg/m^3 while air density is 1.2250 kg/m^3, the difference between the losses are significant. According to the results, without inserting any wedge to the slot openings of the stator the damping loss is as high as 386.2 W while the windage loss is only 0.69 W; with the insertion of the standard wedge to the slots the damping loss is calculated as 362 W while the windage loss is 0.56 W. Hence, it can be concluded that there is a slight difference between the designs without the wedge and the with the standard wedge where the standard wedge design is slightly better. However, creation of a smooth surface by designing a custom wedge that closes the openings and eliminates all the indents, reduces the damping loss significantly to 139.9 W. Also, windage loss is appear as only 0.33 W, which is the lowest windage loss compared to the other two structures.

TABLE IV. DIFFERENT SLOT OPENING STRUCTURES RESULTS AT 3000 RPM

Geometry	Water		Air	
No Wedge	Skin Friction Coefficient (Cd)	0.0251	Skin Friction Coefficient (Cd)	0.0302
	Fluid Density (kg/m^3)	998.2	Air Density (kg/m^3)	1.2250
	Damping Loss (W)	386.2	Windage Loss (W)	0.6900
Standard Wedge	Skin Friction Coefficient (Cd)	0.019	Skin Friction Coefficient (Cd)	0.0245
	Fluid Density (kg/m^3)	998.2	Air Density (kg/m^3)	1.2250
	Damping Loss (W)	362.0	Windage Loss (W)	0.5600
No-Slotting Wedge	Skin Friction Coefficient (Cd)	0.0087	Skin Friction Coefficient (Cd)	0.0142
	Fluid Density (kg/m^3)	998.20	Air Density (kg/m^3)	1.2250
	Damping Loss (W)	139.90	Windage Loss (W)	0.3300

The performed fluid damping loss analyses are done for a 2-pole, 4 kW LS-SynRM. It can be seen from the results that the damping loss has a significant impact on the efficiency as it may go as high as 10% of the machine`s output power. This loss component can be reduced significantly by providing a smooth surface for the fluid to slide between the rotor and stator surfaces. This can be done by customizing the slot wedge structures to avoid indentations on the stator surface. For any case, a CFD analysis should be performed to estimate this loss component for estimating the machine performance and machine dynamics accurately.

IV. CONCLUSION

The submersible water pump motors are fluid-filled and insulated PVC wires usually are preferred as they are suitable for applications where the cables are exposed to fluids. Therefore, the slot openings of the submersible pump motor stators are needed to be larger than industrial motor stators. Although the standard slot wedges are inserted into the slot openings, an indented surface is formed on the stator surface. Since fluid fluctuation is increased with the existence of the indented surface. Hence, the damping loss is increased dramatically. In this study, three slot opening structures with different indents are investigated to put forward that fluid damping loss has a considerable effect on the machine performance and cannot be ignored or assumed as windage loss as in air-cooled machines. A set of computational fluid dynamics finite element analysis is performed to analyze the damping loss in flooded machines for various slot opening structures. The first analysis is performed with a no-wedge and standard wedges are included to the second analysis. It is observed that the design that have smaller indents on the surface performed slightly better than the first design for each speed levels. The highest damping loss for the no-wedge structure is recorded as 386.2 W where it is recorded as 362 W for the standard wedge design. Lastly, a smooth surface with the design of the custom no slotting wedge structure that closes the openings and eliminates all indents is analyzed. According to the results, the design with the custom wedge reduces the damping loss to 139.9 W. As a result of this investigation two important matter is pointed out:

- According to the analysis results it is observed that the damping loss is almost 420 to 650 times of the windage loss for the cases with different stator slot structures investigated in this study. Therefore, fluid damping effect cannot be assumed as windage loss like in the air-cooled motors in flooded motor structures and cannot be ignored for estimating the machine performance accurately.
- Since the exitance of the indents on stator surface increase the damping loss extremely, making the stator inner surface as smooth as possible and eliminating the indents reduces the damping loss of the fluid-filled motors significantly.

ACKNOWLEDGMENT

This research is supported by The Scientific and Technological Research Council of Turkey (TUBITAK) under Grant number 121E413.

REFERENCES

[1] B. Stoffel, "The Role of Pumps for Energy Consumption and Energy Saving," *Assess. Energy Effic. Pumps Pump Units*, pp. 1–24, 2015.

[2] T. A. Lipo, *Introduction to AC Machine Design*. IEEE Press (2017) 193-250.

[3] D. Mingardi and N. Bianchi, "Line-Start PM-Assisted Synchronous Motor Design, Optimization, and Tests," *IEEE Trans. Ind. Electron.*, vol. 64, no. 12, 2017.

[4] D. Mingardi, N. Bianchi, and M. D. Pre, "Geometry of Line Start Synchronous Motors Suitable for Various Pole Combinations," *IEEE Trans. Ind. Appl.*, vol. 53, no. 5, pp. 4360–4367, 2017.

[5] J. J. Lee, S. H. Rhyu, I. S. Jung, and Y. W. Kim, "Design of high efficiency line start permanent magnet motor for submersible pumps," *EEEIC 2016 - Int. Conf. Environ. Electr. Eng.*, pp. 0–3, 2016.

[6] J. Li, J. Song, and Y. Cho, "High performance line start permanent magnet synchronous motor for pumping system," *IEEE Int. Symp. Ind. Electron.*, pp. 1308–1313, 2010.

[7] W. Lyskawinski, C. Jedryczka, and W. Szelag, "Influence of magnet and cage shape on properties of the line start synchronous motor with powder hybrid rotor," *2017 Int. Symp. Electr. Mach. SME 2017*, pp. 1–6, 2017.

[8] B. J. K KOSTKO Associate, A. I. E E Wagner Electric Corp, and S. Louis, "Polyphase reaction synchronous motors; Polyphase reaction synchronous motors," 1923.

[9] C. E. G. Martins, "Design of Synchronous Reluctance Motors With Flux Barriers Using 2D-FEM," 2003.

[10] S. Baka, S. Sashidhar, and B. G. Fernandes, "Multi-barrier two-pole line-start synchronous reluctance motor with high saliency for a bore-well submersible pump," *Proc. IEEE Int. Conf. Ind. Technol.*, vol. 2018-Febru, pp. 475–480, 2018.

[11] M. Villani, M. Santececca, and F. Parasiliti, "High-Efficiency Line-Start Synchronous Reluctance Motor for Fan and Pump Applications," *Proc. - 2018 23rd Int. Conf. Electr. Mach. ICEM 2018*, pp. 2178–2184, 2018.

[12] S. Baka, S. Sashidhar, and B. G. Fernandes, "Design and Optimization of a Two-Pole Line-Start Ferrite Assisted Synchronous Reluctance Motor," *Proc. - 2018 23rd Int. Conf. Electr. Mach. ICEM 2018*, pp. 131–137, 2018.

[13] H. Parveen, U. Sharma, B. Singh, M. Modi, D. Dudharejiya, and C. Jain, "Conversion of Motor Technology for Economical Solar

PV fed Water Pumping System; Conversion of Motor Technology for Economical Solar PV fed Water Pumping System," *2020 Int. Conf. Power, Instrumentation, Control Comput.*, 2020.

[14] S. Baka, S. Sashidhar, and B. G. Fernandes, "Design of an Energy Efficient Line-Start Two-Pole Ferrite Assisted Synchronous Reluctance Motor for Water Pumps; Design of an Energy Efficient Line-Start Two-Pole Ferrite Assisted Synchronous Reluctance Motor for Water Pumps," *IEEE Trans. Energy Convers.*, vol. 36, no. 2, 2021.

[15] D. Tekgun, M. Muhsin Cosdu, B. Tekgun, and I. Alan, "Investigation of the Effects of Multi-Layer Winding Structures in Two Pole Synchronous Reluctance Machines," *Proc. - 2021 IEEE 3rd Glob. Power, Energy Commun. Conf. GPECOM 2021*, pp. 120–125, Oct. 2021.

[16] B. Sarlioglu, "Understanding Electric Motors and Loss Mechanisms Wisconsin Electric Machines and Power Electronics Consortium."